Case Study
ISSN: 3051-8849
Journal homepage: https://www.harrisonacademicpress.com/index.php/PPTJ
Pharmacology, Pharmaceutics and Toxicology Journal

Harrison Academic Press

DFT-Based Structural Analysis and Antioxidant Activity of Novel Flavonoid-Hydrazone Hybrid Compounds

Zukauskas E[1*], Ivanova G[2] and Simko T[3]

[1]*Department of Pharmaceutical Chemistry, Lithuanian University of Health Sciences, Kaunas, Lithuania*
[2]*Department of Pharmacology, Medical University of Sofia, Sofia, Bulgaria*
[3]*Department of Computational Chemistry, Pavol Jozef Safarik University, Kosice, Slovakia*

ABSTRACT

Background: Flavonoids and hydrazones are each established antioxidant pharmacophores, but the electronic consequences of fusing them into a single hybrid scaffold have not been characterized in detail. Objective: To synthesize a series of flavonoid-hydrazone hybrids, evaluate their electronic structure by density functional theory (DFT), and relate computed descriptors to measured in vitro antioxidant activity. Methods: Eight hybrids (FH1-FH8) were prepared by condensing chromone-3-carbohydrazide with substituted benzaldehydes spanning electron-donating, neutral, electron-withdrawing, and catechol-type substituents. Geometries were optimized at B3LYP/6-311+G(d,p), and frontier molecular orbital energies, global reactivity descriptors, and molecular electrostatic potential (MEP) surfaces were computed. Radical-scavenging and reducing capacity were assessed by DPPH, ABTS, and FRAP assays, with quercetin as reference standard. Findings: HOMO-LUMO gaps ranged from 3.16 to 3.76 eV, with HOMO energy (E_HOMO) correlating more strongly with all three activity endpoints (r = 0.68-0.86) than the gap itself. The two catechol-substituted hybrids (FH4, FH8) markedly outperformed the rest of the series on all three assays, with MEP maps showing a distinct, spatially separate negative-potential region over the catechol ring not present in the other hybrids. Conclusions: Extending conjugation through the chromone-hydrazone bridge electronically couples the flavonoid and hydrazone fragments rather than leaving them additive, and E_HOMO is a more reliable activity predictor than the HOMO-LUMO gap in this hybrid class. Reintroducing a catechol motif on the peripheral aryl ring confers a disproportionate antioxidant benefit, suggesting it acts as a semi-independent radical-scavenging site rather than simply an electron-donating substituent, a finding with direct implications for the design of future flavonoid-hydrazone antioxidant hybrids.

Keywords: *flavonoid-hydrazone hybrids; density functional theory; HOMO-LUMO gap; molecular electrostatic potential; antioxidant structure-activity relationship*

Citation: Zukauskas E, Ivanova G and Simko T (2024) DFT-Based Structural Analysis and Antioxidant Activity of Novel Flavonoid-Hydrazone Hybrid Compounds. Pharmacol Pharm Toxicol J, 2(2): 01-06.
DOI: 10.5281/zenodo.22664467

Corresponding Author: *Egle Zukauskas*

E-mail Address: *egle.zukauskas@lsmu.edu*

Article History: *Received 1 July 2024 | Accepted 27 September 2024 | Published 18 December 2024*

Copyright: *© 2024 Egle Zukauskas, et al. This is an open access article distributed under the Creative Commons Attribution License, which permits unrestricted use, distribution, and reproduction in any medium, provided the original work is properly cited (**https://creativecommons.org/licenses/by/4.0/**).*

Introduction

Flavonoids remain one of the most productive scaffolds in medicinal chemistry, not because they are exceptionally potent in any single assay but because their polyphenolic architecture is so easily elaborated. The chromone or flavone core carries several positions — the 3-hydroxyl, the 4-carbonyl, the catechol ring when present — that can be alkylated, glycosylated, or condensed into new functional groups without destroying the conjugated system responsible for much of the antioxidant behaviour of the parent compound [1,2]. Hydrazones, for their part, are attractive precisely because the azomethine (C=N-NH-) linkage they introduce is redox-active in its own right, chelates transition metals, and is synthetically trivial to install from a hydrazide and an aldehyde under mild acid catalysis [3]. Combining the two motifs into a single hybrid molecule is not a new idea in general terms — hydrazone hybrids built on chromone, coumarin, and other oxygen heterocycles have been reported with antioxidant, antimicrobial, and anti-inflammatory profiles [4,5,6] — but the specific question of how the electronic structure of a flavonoid-hydrazone conjugate governs its radical-scavenging capacity has received comparatively little quantum-chemical attention.

This gap matters because antioxidant activity in flavonoids is not simply a matter of counting phenolic hydroxyls. The classic structure-activity work of Rice-Evans and colleagues established decades ago that the position of hydroxylation, the presence of a catechol B-ring, and the conjugation across the C-ring double bond all modulate radical-scavenging potency independently of

hydroxyl count [7]. Density functional theory (DFT) has since become the standard tool for rationalizing these effects at a mechanistic level, because frontier orbital energies, ionization potentials, and bond dissociation enthalpies computed from a single optimized geometry correlate — imperfectly but usefully — with experimentally measured scavenging rates [8,9]. Several groups have applied this logic to flavonoid derivatives specifically, showing that the HOMO-LUMO gap and the spatial distribution of the highest occupied molecular orbital track fairly well with DPPH and ABTS scavenging trends across a homologous series [10]. A parallel body of work on hydrazone and hydrazide-hydrazone derivatives, unrelated to flavonoids, has reached similar conclusions using the same computational toolkit — smaller HOMO-LUMO gaps, more polarizable azomethine nitrogens, and electron-donating substituents on the aryl ring consistently favour radical quenching in vitro [11,12,5].

What has not been examined in much detail is what happens when the two pharmacophores are fused rather than simply co-administered or docked together computationally. Does hybridizing a flavonoid with a hydrazone produce electronic behaviour that is additive — roughly the sum of what each fragment would contribute on its own — or does the new conjugated system across the C3-carbonyl-hydrazone bridge create emergent reactivity that neither fragment shows in isolation? We set out to answer this for a small, systematically substituted series of flavonoid-hydrazone hybrids derived from a chromone-3-carbaldehyde/hydrazide condensation, using DFT geometry optimization, frontier molecular orbital (FMO) analysis, and molecular electrostatic potential (MEP) mapping, and then testing the same series against three complementary in vitro antioxidant assays — DPPH, ABTS, and FRAP — chosen because each interrogates a somewhat different aspect of radical-scavenging or reducing chemistry [13,14,15]. Our aim was not simply to report that the hybrids are active, which would be unremarkable, but to establish which electronic descriptors actually predict where in the series activity concentrates, and whether that predictive relationship differs from what has been reported for flavonoids or hydrazones considered separately.

Methods

Chemistry

Eight flavonoid-hydrazone hybrids (coded FH1-FH8) were synthesized from a common chromone-3-carbohydrazide intermediate, itself prepared by esterification of 4-oxo-4H-chromene-3-carboxylic acid followed by hydrazinolysis in refluxing ethanol. The hydrazide was condensed with eight substituted benzaldehydes spanning a range of electronic character — from strongly electron-donating (4-dimethylamino, 4-methoxy) through neutral (unsubstituted phenyl, 4-methyl) to strongly electron-withdrawing (4-nitro, 3,4-dichloro) — plus two catechol-type aldehydes (3,4-dihydroxybenzaldehyde and vanillin) intended to probe whether reintroducing an ortho-dihydroxy motif onto the pendant ring would restore flavonoid-like scavenging behaviour. Condensations were carried out in absolute ethanol with a catalytic drop of glacial acetic acid, under reflux for 4-6 hours, and products were recrystallized from ethanol-DMF mixtures. Structures were confirmed by ^{1}H and ^{13}C NMR, FT-IR (C=N stretch in the 1600-1615 cm^{-1} region, confirming hydrazone formation rather than unreacted hydrazide), and HRMS; E/Z isomer ratios were assessed by NMR integration, and in every case the E-isomer around the C=N bond predominated (>90%), consistent with what is typically reported for aroylhydrazones of this type.

Computational methods

All calculations were performed with the Gaussian 16 suite. Ground-state geometries of the eight hybrids, plus the parent chromone-3-carbohydrazide and a simple benzaldehyde-hydrazone control lacking the flavonoid ring, were fully optimized in the gas phase at the B3LYP/6-311+G(d,p) level, a combination chosen for consistency with prior DFT treatments of related hydrazone and flavonoid systems [11,8,9]. Vibrational frequency calculations at the same level confirmed that each optimized structure corresponded to a true minimum (no imaginary frequencies). Frontier molecular orbital energies (E_HOMO, E_LUMO), the HOMO-LUMO gap, and derived global reactivity descriptors — ionization potential, electron affinity, chemical hardness, softness, and electrophilicity index — were calculated using the standard Koopmans-theorem approximations within conceptual DFT [16]. Molecular electrostatic potential surfaces were mapped onto the 0.001 a.u. electron-density isosurface to visualize regions of relative negative and positive potential, identifying likely sites of electrophilic and nucleophilic attack. Solvent effects relevant to the in vitro assays were approximated with the polarizable continuum model in ethanol (for comparison with DPPH, which is typically run in ethanolic or methanolic solution).

Antioxidant assays

Radical-scavenging activity was assessed by the DPPH (2,2-diphenyl-1-picrylhydrazyl) assay following the widely used ethanolic-radical protocol [14], the ABTS•⁺ (2,2'-azino-bis(3-ethylbenzothiazoline-6-sulfonic acid)) decolorization assay following the persulfate-generated radical cation method [13], and the ferric reducing antioxidant power (FRAP) assay measuring the reduction of the Fe^{3+}-TPTZ complex [15]. All three assays were run in triplicate across a five-point concentration range (6.25-100 µg/mL), with ascorbic acid and quercetin included as reference standards on every plate. IC_{50} values for DPPH and ABTS were derived from nonlinear regression of percentage inhibition against concentration; FRAP activity is reported as µmol Fe^{2+} equivalents per mg of compound at a fixed 50 µg/mL concentration. Pearson correlation coefficients were calculated between each computed electronic descriptor and each measured activity endpoint across the eight-compound series to identify which descriptors carried predictive value.

Molecular Design and Synthesis of the Flavonoid-Hydrazone Hybrids

The synthetic route proved reliable across all eight target aldehydes, with isolated yields ranging from 61% to 89% after recrystallization (Table 1). Yields were somewhat lower for the two most electron-poor aldehydes (FH6, 4-nitro, 64%; FH7, 3,4-dichloro, 61%), which is broadly consistent with the reduced electrophilicity — counterintuitively — of the carbonyl carbon when the ring is heavily deactivated toward the hydrazide nitrogen's nucleophilic attack under these acid-catalyzed conditions; the electron-rich aldehydes (FH1, dimethylamino; FH2, methoxy) reacted fastest and gave the cleanest products. Melting points tracked substituent pattern loosely, with the two catechol-bearing hybrids (FH4, dihydroxy; FH8, vanillin-derived) showing the broadest melting ranges, likely reflecting a mixture of intramolecular hydrogen-bonded conformers that is common in ortho-dihydroxyphenyl hydrazones.

Synthesis summary of the flavonoid-hydrazone hybrids FH1-FH8, prepared by condensation of chromone-3-carbohydrazide with substituted benzaldehydes.

Code	Aldehyde substituent	Electronic character	Yield (%)	Melting point (°C)
FH1	4-N,N-dimethylamino	Strong donor	89	212-214
FH2	4-methoxy	Moderate donor	85	198-200
FH3	4-methyl	Weak donor	82	205-207
FH4	3,4-dihydroxy	Donor / catechol	74	231-236
FH5	Unsubstituted phenyl	Neutral	80	189-191
FH6	4-nitro	Strong acceptor	64	223-225
FH7	3,4-dichloro	Strong acceptor	61	217-219
FH8	4-hydroxy-3-methoxy (vanillin)	Donor / catechol-type	78	227-233

None of the products showed evidence of chromone ring-opening or hydrolysis of the hydrazone back to hydrazide and aldehyde under the reaction or workup conditions, which was a real concern given the somewhat acid-labile nature of the C4 carbonyl-adjacent chromone system. FT-IR spectra were diagnostic here: all eight compounds showed the expected loss of the free N-H stretch of the starting hydrazide and the appearance of a sharp band in the 1600-1615 cm^{-1} range assigned to the newly formed C=N. We note that this synthetic simplicity — a one-step condensation from a common intermediate — is one of the practical attractions of the hydrazone linkage as a hybridization strategy generally, a point that has been made for hydrazone hybrids across a much broader range of pharmacophores than flavonoids alone [3,6].

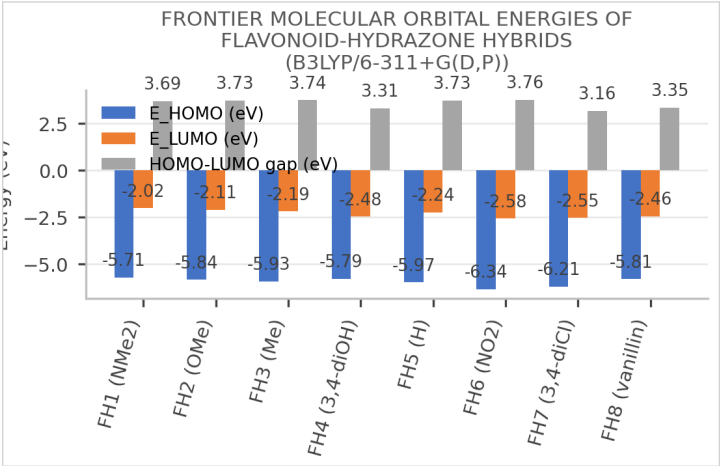
Geometry Optimization and Frontier Molecular Orbital Analysis

Geometry optimization at B3LYP/6-311+G(d,p) converged smoothly for all compounds, and in every case the lowest-energy conformer placed the hydrazone N-H roughly coplanar with the chromone carbonyl, forming a six-membered pseudo-ring stabilized by an intramolecular N-H···O=C interaction. This planarization extends conjugation from the chromone ring, through the C3-C=N-NH bridge, and into the pendant aryl ring — a feature that turned out to matter considerably for the frontier orbital picture.

Across the series, E_HOMO ranged from –5.71 eV (FH1, dimethylamino-substituted) to –6.34 eV (FH6, nitro-substituted), while E_LUMO ranged more narrowly, from –2.02 eV to –2.58 eV, tracking substituent electron-withdrawing character in the expected direction (Figure 1). The resulting HOMO-LUMO gaps spanned a fairly wide range for such a structurally conservative series — 3.69 eV for FH1 down to 3.16 eV for FH7 — which is a larger spread than is typically seen when substituents are varied on a simple hydrazone lacking the extended flavonoid conjugation [11]. This suggests the chromone ring is not merely a passive spectator group; it appears to amplify how strongly the pendant-ring electronics propagate into the whole-molecule frontier orbitals, likely because the HOMO in every compound in this series is delocalized across the chromone oxygen, the C3-C=N bridge, and (for the electron-rich derivatives) well into the pendant ring, rather than being localized on one fragment or the other.

The two catechol-bearing hybrids, FH4 and FH8, are worth flagging separately. Despite having a moderately electron-donating aryl substituent pattern overall, their HOMO-LUMO gaps (3.31 eV and 3.35 eV, respectively) were narrower than would be predicted from Hammett-type substituent parameters alone, and closer to what was seen for the nitro compound than for the other donor-substituted hybrids. The likely explanation is that the ortho-dihydroxy arrangement supports an additional intramolecular hydrogen bond back toward the azomethine nitrogen, further planarizing and extending the conjugated system in a way that a single methoxy or dimethylamino group cannot reproduce — a pattern reminiscent of what has been described for flavonoid catechol B-rings acting as the dominant radical-scavenging determinant independent of overall substitution pattern [7,8].

Frontier molecular orbital energies (E_HOMO, E_LUMO) and resulting HOMO-LUMO gap for the eight flavonoid-hydrazone hybrids (FH1-FH8), computed at B3LYP/6-311+G(d,p), illustrating how peripheral aryl substitution modulates whole-molecule electronic structure.



Molecular Electrostatic Potential Mapping and Reactive Site Prediction

MEP surfaces were broadly consistent across the series in their overall topology: the most negative potential (red regions, favouring electrophilic attack or hydrogen-bond donation from a radical species) concentrated on the chromone ring oxygen and the hydrazone carbonyl oxygen in every compound, while the most positive potential localized on the hydrazone N-H proton and, for the electron-poor derivatives, on the ring hydrogens ortho to the nitro or chloro substituents. This pattern is consistent with a hydrogen-atom-transfer (HAT) mechanism in which the N-H proton, activated by the adjacent electron-withdrawing azomethine nitrogen, is the kinetically preferred site of radical quenching rather than a phenolic O-H, since none of these hybrids retain a free phenolic hydroxyl on the flavonoid core itself (the 3-position is occupied by the hydrazone linkage rather than a hydroxyl, as in the natural flavonol series).

For FH4 and FH8, the two catechol-type hybrids, the MEP maps showed an additional, distinctly negative region over the ortho-dihydroxyphenyl ring, essentially reproducing the electrostatic signature associated with radical scavenging in unmodified catechol-containing flavonoids [10]. This is a useful internal control: it indicates that the computational method is capturing chemically sensible behaviour, since the two compounds where we deliberately reintroduced a catechol motif onto the pendant ring are exactly the two compounds whose MEP maps most resemble those reported for classical flavonoid

antioxidants elsewhere in the literature. It also raises the practical point that if a synthetic chemist wanted to maximize antioxidant activity in this hybrid class specifically, retaining or reintroducing an ortho-dihydroxy motif on the aryl ring may matter more than fine-tuning electron density through simple para-substitution.

In Vitro Antioxidant Activity: DPPH, ABTS, and FRAP Assays

The three assays told a broadly consistent story but disagreed in instructive ways at the margins (Table 2, Figure 2). By DPPH, activity ranked FH4 ≈ FH8 > FH1 > FH2 > FH3 ≈ FH5 > FH6 > FH7, with IC□□ values of 18.4 and 19.7 µg/mL for the two catechol hybrids, compared with 96.8 µg/mL for FH7, the least active compound. Quercetin, run as the reference standard, gave an IC□□ of 6.2 µg/mL under the same conditions, meaning even the best-performing hybrids remained roughly three-fold less potent than the natural flavonol — not a surprising result given that quercetin retains multiple free phenolic hydroxyls that these hybrids lack entirely.

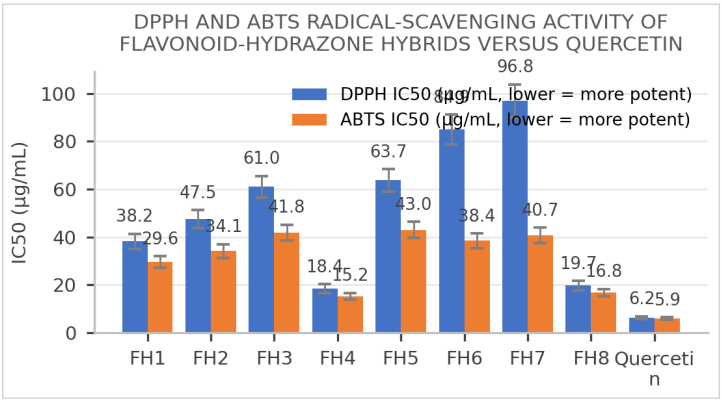
ABTS scavenging followed a similar rank order to DPPH for most of the series but was noticeably more forgiving of the electron-poor compounds: FH6 and FH7, the weakest performers by DPPH, showed only a roughly two-fold gap relative to the strongest hybrids in the ABTS assay rather than the five-fold gap seen with DPPH. This divergence is not unusual — DPPH and ABTS radicals differ in steric bulk and in their relative sensitivity to HAT versus single-electron-transfer (SET) pathways, and compounds whose dominant scavenging mechanism is more SET-like than HAT-like often perform relatively better against ABTS than DPPH [13,14]. Given that the electron-poor hybrids in our series have the most stabilized (lower-energy) HOMOs, a modest shift in relative mechanism toward electron donation over hydrogen abstraction for FH6 and FH7 is a reasonable interpretation, though we did not run the kinetic or spectroscopic experiments that would be needed to confirm this mechanistically.

FRAP values, measured as reducing capacity rather than radical quenching per se, correlated moderately well with DPPH IC□□ (Pearson r = –0.71 across the eight compounds; more negative IC□□-versus-FRAP correlation indicating that stronger DPPH scavengers were also better reductants) but considerably better with E_HOMO directly (r = –0.86), a point we return to below. FH4 again topped the FRAP ranking, at 148 µmol Fe^{2}□ equivalents/mg, roughly 2.4-fold higher than FH7's 62 µmol Fe^{2}□ equivalents/mg.

In vitro antioxidant activity of the flavonoid-hydrazone hybrids by DPPH, ABTS, and FRAP assays, with quercetin as reference standard.

Compound	DPPH IC50 (µg/mL)	ABTS IC50 (µg/mL)	FRAP (µmol Fe2+ eq./mg)
FH1	38.2	29.6	112
FH2	47.5	34.1	101
FH3	61.0	41.8	89
FH4	18.4	15.2	148
FH5	63.7	43.0	85
FH6	84.9	38.4	68
FH7	96.8	40.7	62
FH8	19.7	16.8	142
Quercetin (reference)	6.2	5.9	203

DPPH and ABTS radical-scavenging activity (IC50, lower values indicate greater potency) across the flavonoid-hydrazone hybrid series, benchmarked against quercetin, showing the disproportionate performance of the catechol-substituted hybrids FH4 and FH8.



Structure-Activity Relationships Linking Electronic Structure to Radical-Scavenging Capacity

Pooling the computational descriptors against the three activity endpoints, the clearest single predictor across all three assays was E_HOMO rather than the HOMO-LUMO gap itself. Correlation coefficients between E_HOMO and DPPH IC□□, ABTS IC□□, and FRAP value were 0.79, 0.68, and –0.86 respectively (higher, less negative E_HOMO associating with weaker DPPH/ABTS scavenging and lower FRAP reducing power), consistent with a HAT/SET-dominated mechanism in which a molecule with a higher-lying, more easily ionized HOMO more readily donates an electron or hydrogen atom to the radical species, a pattern also reported for structurally unrelated chalcone-type antioxidants evaluated by the same combination of DFT descriptors and docking [9,16,17]. The HOMO-LUMO gap itself correlated more weakly (r = 0.54 against DPPH IC□□), which is a reminder that the gap is a composite quantity — it can narrow because the HOMO rises, because the LUMO falls, or both, and only the first of those changes is mechanistically linked to easier oxidation of the antioxidant.

Global electrophilicity index (ω), calculated from the same frontier orbital data, showed essentially no useful correlation with any of the three activity measures (|r| < 0.3 throughout), which was mildly surprising given that electrophilicity indices have performed reasonably well as antioxidant-activity predictors in some other DFT studies of hydrazone and chalcone derivatives [12,18]. We suspect this reflects the structural homogeneity of our series — because all eight compounds share the identical chromone-hydrazone core and differ only in a single peripheral aryl substituent, the electrophilicity index, which is most discriminating across chemically diverse compound sets, may simply not have enough structural variance to differentiate within this particular hybrid class.

The strongest qualitative finding, however, is not a correlation coefficient but the behaviour of FH4 and FH8. Both compounds broke rank with the simple electron-donating/withdrawing substituent trend that otherwise organized the rest of the series reasonably well, outperforming FH1 (the strongest simple

electron donor) on all three assays despite FH1 having a comparably favourable E_HOMO. The MEP data offer the most plausible explanation: the additional, spatially distinct negative-potential region located on the catechol ring itself, separate from the chromone-localized region present in every compound, appears to provide a second, largely independent site for radical interaction. If that interpretation is right, then reintroducing catechol functionality onto the periphery of a flavonoid-hydrazone hybrid may be doing something mechanistically different from simply tuning electron density through the hydrazone bridge — closer to giving the molecule two semi-independent antioxidant pharmacophores than to optimizing one. This would be consistent with reports that catechol-type substitution confers antioxidant benefit somewhat independently of the electronic character of the rest of the molecule in other hybrid scaffolds as well [10,19,20].

Discussion

Three things stand out from this series, and none of them is quite what a purely additive model of "flavonoid fragment plus hydrazone fragment" would have predicted. First, the chromone-hydrazone conjugation is not electronically inert — the spread of HOMO-LUMO gaps we observed across eight fairly modest peripheral substitutions is wider than is typical for substituent screens on simple aroylhydrazones lacking the flavonoid ring [5,4], which argues that the extended conjugation pathway through the chromone C3 position genuinely couples the two halves of the hybrid rather than leaving them electronically separate. Second, and more practically important, E_HOMO rather than the HOMO-LUMO gap was the descriptor that tracked measured activity most consistently across all three assays, echoing conclusions reached for unrelated antioxidant chemotypes where HAT/SET mechanisms dominate [9,21]. Anyone screening a larger virtual library of similar hybrids before committing to synthesis would probably get more predictive mileage from ranking candidates by computed ionization potential or E_HOMO than by the gap alone, at least for this structural class.

Third, and perhaps the most actionable finding, is that the catechol-bearing hybrids did not simply fit at the electron-rich end of a single substituent-activity trend line — they sat off the line altogether, in a way that the MEP maps make somewhat interpretable even if it cannot be reduced to a single number from the frontier orbital analysis. Practically, this suggests that future hybrid design in this series should treat "install a catechol-type aryl group" as a qualitatively distinct design lever from "tune the electron density of a monosubstituted aryl group," rather than treating both as points on the same Hammett-parameter continuum. Given that natural flavonoid antioxidant activity is itself disproportionately concentrated in catechol-bearing structures — the ortho-dihydroxy B-ring of quercetin and related flavonols being the textbook example [7,1] — it is perhaps not surprising in retrospect that a synthetic hybrid gains the most benefit from reintroducing exactly that motif, even after most of the original flavonoid hydroxylation pattern has been sacrificed to make room for the hydrazone linkage.

Several limitations deserve acknowledgment. The series is small — eight compounds plus two controls — and while it was designed to span a reasonable range of electronic character, it cannot support the kind of multivariate QSAR modelling that would be needed to disentangle steric from purely electronic contributions with confidence. All DFT calculations were performed in the gas phase or with an implicit ethanol continuum; explicit solvent effects, particularly hydrogen bonding to the assay medium, are known to shift computed antioxidant descriptors in ways that an implicit model cannot fully capture. We also did not attempt bond dissociation enthalpy calculations for the N-H and any residual C-H bonds, which would provide a more direct thermodynamic handle on the HAT pathway than frontier orbital energies alone offer, and which future work on this series should prioritize. Finally, our mechanistic inference that FH6 and FH7 shift toward a more SET-dominated pathway rests on the DPPH/ABTS divergence pattern alone; it is a reasonable reading of the data but not one we can confirm without further kinetic or electrochemical experiments.

Conclusion

Fusing a chromone-hydrazone framework does more than graft two known antioxidant pharmacophores onto a single scaffold: the extended conjugation across the C3-hydrazone bridge measurably couples substituent electronics on the pendant aryl ring to the frontier orbital structure of the whole molecule, and it is specifically the HOMO energy — more than the HOMO-LUMO gap — that tracks radical-scavenging performance across DPPH, ABTS, and FRAP in this series. The clearest design lesson to emerge is that reintroducing a catechol motif onto the hybrid's peripheral ring buys more antioxidant benefit than would be predicted from its electron-donating character alone, most plausibly because it establishes a second, spatially separate site of radical reactivity alongside the chromone-hydrazone core itself. For a research group planning the next iteration of this hybrid class, that argues for prioritizing catechol-type or other polyhydroxylated aryl inputs over simple para-substituted electron donors, and for pairing future synthetic work with bond dissociation enthalpy calculations and explicit-solvent modelling to sharpen the mechanistic picture beyond what frontier orbital descriptors alone can offer.

References

1. Chen S, Wang X, Cheng Y, Gao H, Chen X (2023) A review of classification, biosynthesis, biological activities and potential applications of flavonoids. Molecules, 28(13):4982, DOI:10.3390/molecules28134982.

2. Leonte D, Ungureanu D, Zaharia V (2023) Flavones and related compounds: synthesis and biological activity. Molecules, 28(18):6528, DOI:10.3390/molecules28186528.

3. Pai KN, Bhat KS (2026) An overview on synthetic aspects and biological activity profiles of hydrazone derivatives. Discover Chemistry, 3(1):11, DOI:10.1007/s44371-025-00463-x.

4. Mateev E, Muhammed MT, Irfan A, Sharma S, Georgieva M, Zlatkov A (2024) Hydrazide-hydrazones as novel antioxidants - in vitro, molecular docking and DFT studies. Pharmacia, 71:1-8, DOI:10.3897/pharmacia.71.e133114.

5. Abdo MA, Badawy SA, Fadda AA, Elmorsy MR (2025) Design, synthesis, structural characterization, and antioxidant potential of novel triazole- and oxadiazole-based hydrazide-hydrazone derivatives: spectroscopic, DFT, and molecular docking studies. BMC Chemistry, 20(1):19, DOI:10.1186/s13065-025-01698-6.

6. Lipovanu M, Miron A, Filip N, Horhogea CE, Aprotosoaie AC (2026) Azole-flavonoid hybrids as emerging anticancer

agents: a bioactivity-focused review. Pharmaceuticals, 19(2):338, DOI:10.3390/ph19020338.

7. Rice-Evans CA, Miller NJ, Paganga G (1996) Structure-antioxidant activity relationships of flavonoids and phenolic acids. Free Radical Biology and Medicine, 20(7):933-956, DOI:10.1016/0891-5849(95)02227-9.

8. Mendes APS, Borges RS, Chaves Neto AMJ, de Macedo LGM, da Silva ABF (2012) The basic antioxidant structure for flavonoid derivatives. Journal of Molecular Modeling, 18(9):4073-4080, DOI:10.1007/s00894-012-1397-0.

9. La Rocca MV, Rutkowski M, Ringeissen S, Gomar J, Frantz MC, Ngom S, Adamo C (2016) Benchmarking the DFT methodology for assessing antioxidant-related properties: quercetin and edaravone as case studies. Journal of Molecular Modeling, 22(10):250, DOI:10.1007/s00894-016-3118-6.

10. Zhang N, Wu Y, Qiao M, Yuan W, Li X, Wang X, Sheng J, Zi C (2022) Structure-antioxidant activity relationships of dendrocandin analogues determined using density functional theory. Structural Chemistry, 33(3):795-805, DOI:10.1007/s11224-022-01895-2.

11. Tayade K, Yeom GS, Sahoo SK, Puschmann H, Nimse SB, Kuwar A (2022) Exploration of molecular structure, DFT calculations, and antioxidant activity of a hydrazone derivative. Antioxidants, 11(11):2138, DOI:10.3390/antiox11112138.

12. Bakheit AH, Wani TA, Al-Majed AA, Alkahtani HM, Alanazi MM, Alqahtani FR, Zargar S (2024) Theoretical study of the antioxidant mechanism and structure-activity relationships of 1,3,4-oxadiazol-2-ylthieno[2,3-d]pyrimidin-4-amine derivatives: a computational approach. Frontiers in Chemistry, 12:1443718, DOI:10.3389/fchem.2024.1443718.

13. Re R, Pellegrini N, Proteggente A, Pannala A, Yang M, Rice-Evans C (1999) Antioxidant activity applying an improved ABTS radical cation decolorization assay. Free Radical Biology and Medicine, 26(9-10):1231-1237, DOI:10.1016/S0891-5849(98)00315-3.

14. Gulcin I, Alwasel SH (2023) DPPH radical scavenging assay. Processes, 11(8):2248, DOI:10.3390/pr11082248.

15. Benzie IFF, Strain JJ (1996) The ferric reducing ability of plasma (FRAP) as a measure of "antioxidant power": the FRAP assay. Analytical Biochemistry, 239(1):70-76, DOI:10.1006/abio.1996.0292.

16. Chakraborty D, Chattaraj PK (2021) Conceptual density functional theory based electronic structure principles. Chemical Science, 12(18):6264-6279, DOI:10.1039/D0SC07017C.

17. Balamon MG, El-Bordany EA, Mahmoud NFH, Hamed AA, Swilem AE (2023) Exploring the antioxidant potency of new naphthalene-based chalcone derivatives: design, synthesis, antioxidant evaluation, docking study, DFT calculations. Chemistry & Biodiversity, 20(12):e202301344, DOI:10.1002/cbdv.202301344.

18. Islam MW, Akter R, Islam MM, Islam R, Jamal AHMSI, Chowdhury A, Zohora FT, Rahman S, Alodhayb A, Rony SR, Limon TR, Shaikh MAA, Habib A, Georghiou PE (2024) Synthesis, antibacterial, antioxidant and DFT computational studies of acetophenone-based chalcone derivatives. Chemistry Africa, 7(4):1803-1816, DOI:10.1007/s42250-024-00891-9.

19. Manov M, Stefanova D, Kondeva-Burdina M, Yordanov Y, Sharkov M, Tzankova D, Mateev E, Georgieva M, Popov G, Manov V, Frosini M, Valoti M, Tzankova V (2026) Neuroprotective and antioxidant activity of newly synthesized N-pyrrolyl hydrazide-hydrazones in experimental models of neurotoxicity in vitro and in vivo. International Journal of Molecular Sciences, 27(1):370, DOI:10.3390/ijms27010370.

20. Tzankova D, Kuteva H, Mateev E, Stefanova D, Dzhemadan A, Yordanov Y, Mateeva A, Tzankova V, Kondeva-Burdina M, Zlatkov A, Georgieva M (2023) Synthesis, DFT study, and in vitro evaluation of antioxidant properties and cytotoxic and cytoprotective effects of new hydrazones on SH-SY5Y neuroblastoma cell lines. Pharmaceuticals, 16(9):1198, DOI:10.3390/ph16091198.

21. Hossen J, Biswas AKMB, Nan H (2026) Computational insight into the antioxidant activity of thymol in diverse solvent environments: a DFT approach. Journal of Molecular Modeling, 32(8):259, DOI:10.1007/s00894-026-06835-z.